

Sulphate Ions Removal from an Abandoned Mine Water using Electrocoagulation. Characterization of the Flocs Originated through Chemical and Morphological Analysis

Brett González-Cárdenas¹, Gilberto Carreño-Aguilera^{1,*}, María J. Puy-Alquiza²,
Raúl Miranda-Avilés², Araceli Jacobo-Azuara³

¹ Departamento de Ingeniería Geomática e Hidráulica, Universidad de Guanajuato, Av. Juárez 77, Zona Centro, C.P. 36000, Guanajuato, Guanajuato, México

² Departamento de Ingeniería en Minas, Metalurgia y Geología, Universidad de Guanajuato, Ex Hacienda de San Matías S/N, San Matías, San Javier, 36020 Guanajuato, Guanajuato, México.

³ Departamento de Química, Universidad de Guanajuato, Norial Alta S/N, 36050 Guanajuato, Guanajuato, México.

*E-mail: gca@ugto.mx

Received: 13 March 2019 / Accepted: 5 May 2019 / Published: 10 June 2019

This paper shows a study on the removal of sulphate ions from the abandoned mine drainage by applying the electrocoagulation process. The aluminum plates were used as a sacrificial electrode in a filter-type reactor on different volumetric flows between 0.1 and 0.4 L min⁻¹, and the current densities of 4, 5, 6 and 7 mA/cm². 60 L of water were used, extracted from the “El Nopal” mine, which is located in the city of Guanajuato, Mexico ([SO₄²⁻] = 6704 mg L⁻¹, pH=8.2, conductivity= 3.72 mS cm⁻¹), collected during the January - July 2018 period. The concentration of sulphate ions decreased from 6704 mg L⁻¹ to 1871 mg L⁻¹ (obtaining 72% of removal), using a current density of 4 mA cm⁻² and a linear velocity of 2.95 cm s⁻¹. After that, to the residues generated by the electrocoagulation process (flocs) we performed the analyses of SEM-EDS, XRD, Infrared Spectroscopy and Magnetic Resonance with the purpose to learn about their chemical composition, crystalline structure and functional groups present in the flocs, respectively, indicating that in the said composition there were found chemical elements like O, Na, Mg, Al, Si, S, Cl, K and Ca.

Keywords: Sulphate removal, Abandoned mine water, Electrocoagulation, Flocs, Aluminum sacrificial anode.

1. INTRODUCTION

The quality of life of the population depends to a great extent on the access to the goods required for their survival and development; the treatment of both drinking water and wastewater is of great importance in order to reduce the mortality rate and generate a higher life expectancy for the population,

by preventing the spread of diseases related to the lack of sanitation and health. Mining is one of the industrial activities with the highest degree of water handling, because on the one hand, it employs water in a great number of operations, and on the other hand, through its excavation work, it generates large volumes fundamentally by infiltration of the intercepted aquifers and the superficial runoff. The mining exploitations provoke certain hydrological effects on underground or superficial waters being the principal decrease of water quality, making it unsuitable for human consumption and other uses. The contamination of mining water is generally due to the introduction of substances or some particular forms of energy, like heat that leads to changes in its physical and chemical properties. When in contact with air, mine waters create a great number of problems due to the production of chemical and biological oxidations of sulphides [1]. The mines drainage contains a large amount of suspended solids with a high content of sulphate and metals (Fe, Al, Mn, Zn, Cu, Pb, Cd) with hundreds of milligrams per liter. These elements at high concentrations are dangerous for biological activity; they pollute watercourses and may cause damage to the structures built by men [2].

The sulphides oxidation is the main factor that contributes to the introduction of the sulphates into water flows, when those mines drains come into contact with superficial water bodies; the biotic impacts are generated in the organisms contained in water flows and lakes. Furthermore, there is the habitat alteration due to the contact with precipitated metals, interruptions with the cycles of nutrients, corrosion and implications on the population's health. Very often, water becomes inadequate for domestic, agricultural and industrial uses (the limit concentration of sulphate ions in water for the human consumption established by the World Organization of Health is 250 mg L^{-1}) [3-7]. One of the most important ions in the mines drainage is the sulphate ion (SO_4^{-2}); since the most probable natural sources are the dissolution of evaporates that minerals may contain, such as gypsum or anhydrite, which belong to the sulphate group; as well, weathering of minerals of the sulfide group contained in the countless veins and grains of the region or located in the deposits of massive sulphides, which through the hydrolysis reactions form sulphate ions and volcanic activity in the form of gases and/or hydrothermalism rich in species of the reduced (H_2S , HS^- , S^{-2}) or oxidized sulfurs (SO_2 , SO_3 , SO_4^{-2}). This natural pollution might also cause acid drainage possibly of smaller magnitude, but of larger extension [8].

In the mining district of Guanajuato, the drainage lines are mostly not acid, because the biggest part of the pH is slightly alkaline (pH average 7.1-8.3). Nevertheless, the values of high concentration of sulphate ions could indicate that they exist, as generally low values of pH stay close to the contamination source due to hydrolysis reactions of silicate, since water tends to be in equilibrium with the atmospheric CO_2 , what leaves the residual evidence of an increase of the sulphate ions concentration. Another reason for water alkalinity could be the quantity of the dissolved calcite, since the presence of carbonate ions (CO_3^{-2}) would tend to increase the pH [8].

2. EXPERIMENTATION

2.1 Water samples

Water used for this project was taken from the experimental mine "El Nopal", located along the panoramic highway in the municipality of Guanajuato (latitude 21.032509° , longitude: -101.259221° ,

height SNM 2084 m); the initial works in this mine started with mining metals like gold, silver, copper and zinc at the beginning of 1868, and they stopped working forty years later [9].

The characteristics of the mine water taken for electrocoagulation testing were: $[\text{SO}_4^{-2}] = 6704 \text{ mg L}^{-1}$, $\text{pH}=8.2$, conductivity 3.72 mS cm^{-1} , the composition of the types of sulphates contained were (% of the whole mass): CaSO_4 : 29.5, CuSO_4 : 0.07, SrSO_4 : 0.37, MgSO_4 : 67.03, K_2SO_4 :3.03.

2.2 Electrocoagulation reactor

The reactor was made of two plates of high-density polypropylene; the reactor assembly was done with a single pole configuration, in which five aluminum electrodes were used as anodes and four as cathodes. Both sides of the anodes were used in a manner that the working area was increased. Silicone separators were employed between each pair of electrodes, in order to form a channel of a serpentine shape, which induced to a turbulent flow on the passage of water being treated; that was done for improving the transportation of anode coagulant mass to the solution, avoiding the electrode passivation (see Figure 1). Table 1 shows the reactor dimensions.

Table 1. Electrocoagulation reactor dimensions.

| | Reactor |
|--|---------------------|
| Volume, V (cm^3) | 108.16 (BT×L×ST) |
| Height, B (cm) | 2.6 |
| Chanel width, S (cm) | 0.65 |
| Channel length, L (cm) | 8.0 |
| Number of channels | 8 |
| Total length, LT (cm) | 64.0 |
| Anode area in each channel (cm^2) | 20.8 |
| Cathode area in each channel (cm^2) | 20.8 |

The EC reactor was joined to a hydraulic system that consists of a pump magnetically coupled on 1/10 hp (Little Giant 4-MD-HC model), which was used to supply the solution flow (see Figure 1). To measure the volumetric flow, a flow meter of $0.1 - 1.0 \text{ L min}^{-1}$ White Industries model F44250 was used. The pipes, valves and connections were made of PVC. The pipes that connect the deposit (water supply) with the pump were of 0.50 inches in diameter. A power supply with BK precision model 1665 was used to carry out the electrolysis testing. The cell potential was registered directly by the power supply indicator.

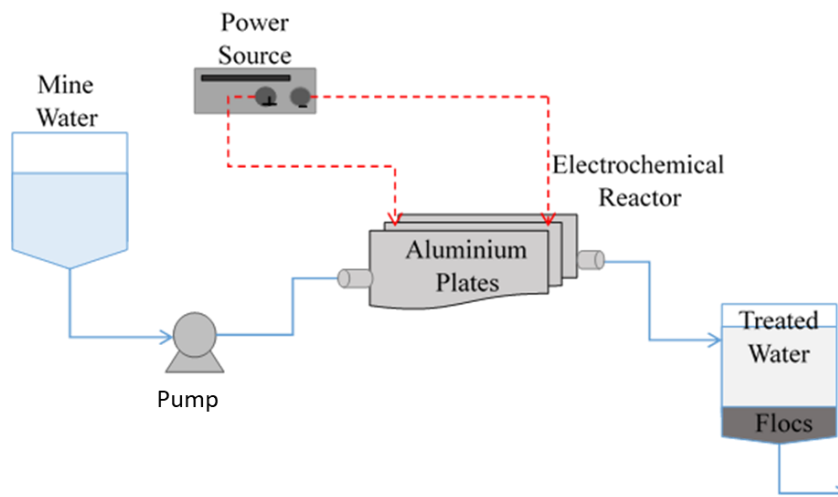


Figure 1. Flow and electric circuit for the electrocoagulation process using a filter-press type reactor.

2.3 Methodology

The electrocoagulation tests were performed under different hydrodynamic conditions given by the volumetric flow ($0.1\text{--}0.4\text{ L min}^{-1}$), producing flow velocities between 0.98 and 2.90 cm s^{-1} . Four different current densities were employed here: 4 , 5 , 6 and 7 mA/cm^2 . In order to avoid the passivation of aluminum electrodes, the pH of the sample was adjusted to 7 with HCl to 1.5% ; to this value of pH, all the experiments presented in this work were done.

To each water sample produced by EC, the jars testing was performed in order to stimulate the flocculation; the said tests were carried out at 40 rpm during 15 minutes each one. In what refers to the adsorption of the sulphate ions over the aluminum flocs, once these aggregates were precipitated (1 hr), the residual sulphate concentration of the treated solutions and the analysis of the flocs were analyzed.

2.3.1 Analytical procedure

The concentration of sulphate ions in water samples were quantified through the gravimetric technique by UV-Visible Spectroscopy, according to the Mexican Official Standard NMX-AA-74-1981, employing ultraviolet-visible Spectrophotometer model UV-2401 PC of Shimadzu brand and with UV-probe software and a reading range of 900 to 190 nm .

Both the pH and the conductivity were measured on a pH-meter model Thermo Scientific Orion Versa, employing electrodes for the conductivity and for the pH of Orion brand.

The concentration of aluminum was determined by dissolving the flocs and using HCl concentrate, and later, analyzed on a Spectrometer of Atomic Absorption model AAnalyst 200 of Perkin Elmer brand.

The analysis through the scanning electron microscope (SEM) was carried out using a SEM Jeol JSM-6010PLUS / LA, integrated within an Energy Dispersive X-ray Spectrometer (EDS). The analysis of the samples was performed in low vacuum.

The analysis of the X-ray diffraction (XRD) of the flocs, formed during the electrocoagulation process, was carried out in an X-ray diffractometer of Rigaku brand model Ultima IV with a Bragg-Brentano geometry (BB) and a scintillation detector (SC) with copper tube with wavelength CuK 1.54 Å, at a speed of 5 degrees min⁻¹ (sp5), current 30 mA and acceleration voltage 30V, goniometer arm 2T and 0.3mm measurement steps.

The analysis through infrared spectrometry was carried out by means of an Infrared Spectrometer with the Fourier FTIR-ATR transforms, model TENSOR 27, brand BRUKER, software OPUS V 6.5, reading range 4000- 400 cm⁻¹ (medium IR).

The samples were analyzed with a Spectrometry of X-ray Fluorescence NEX CG, using dispersion energy (EDXRF). The spectrometer has an X-ray Tube of Pd anode with a maximum power of 50W and a maximum voltage of 50kV -2mA and in the He atmosphere.

In addition, to complement of the characterization of flocs, the aluminum coordination in the flocs structure was determined by the Nuclear Magnetic Resonance of Solids (RMNS) for ²⁷Al. The analysis by RMNS was carried out using a spectrometer model Avance III HD of Bruker brand 400 MHz.

3. RESULTS AND DISCUSSION

There are different technologies for the removal of sulphate ions contained in water, such as ionic exchange, lime treatment, precipitation, adsorption, filtration, electrocoagulation (see Table 2); several of these technologies are combined with the chemical coagulation processes [10-14].

Table 2. Characteristics of different methods of removal of sulphate ions contained in water.

| Method | Characteristics | References |
|--------------------|---|--------------------|
| Ion exchange | <ul style="list-style-type: none"> • Reversible process and • Capacity is limited • The resin must be regenerated | [15-17] |
| Lime treatment | <ul style="list-style-type: none"> • Hydroxides precipitates are formed with metals • Large quantities of sludge are produced | [18] |
| Precipitation | <ul style="list-style-type: none"> • Most of the sludge components can be recovered | [19-20] |
| Adsorption | <ul style="list-style-type: none"> • A little expensive • Modeling can be done using isotherms | [21-23] |
| Filtration | <ul style="list-style-type: none"> • Produced sludge can be used as an alternative for lime pre-treatment • Limited lifetime • High removal efficiency | [24-25] |
| Electrocoagulation | <ul style="list-style-type: none"> • Less sludge is produced than those generated by chemical coagulation • Passivation of the electrodes is generated | [26-31, this work] |

The sulphate ions can be removed with weak base anionic resins (i.e. Amberlyst A21) [15]. The affinity of the most common ions for the resin used in the ion exchange has the following sequence: citrate > SO_4^{2-} > NO_3^- > I^- > Br^- > Cl^- > formate > acetate > F^- [16]. Because the capacity and selectivity of the resins cannot be considered as ion exchange as a principal technique of sulphate removal, but as a complementary technique to chemical precipitation [17].

The application of lime treatment has been used profitably to remove sulphates from contaminated water; the effectiveness of the process depends mainly on the low solubility, and therefore, on the metal hydroxides contained in contaminated water [18].

Gypsum precipitation is a method that has been used effectively for the removal of sulphates contained in mine water due to the simplicity of the process and tolerance to temperature fluctuations [19]. It has been shown that precipitation with ettringite ($Ca_6Al_2(SO_4)_3(OH)_{12} \cdot 26H_2O$) has been able to reduce the concentration of the said ions up to 200 mg L^{-1} [20].

The removal of sulphates has been studied with a variety of materials, for example, activated carbon modified with polypyrrole [21], which generated a positive surface charge that offers a high capacity of aggregation; likewise, modified zeolites have been used, for example, with neighborhood [22]. The capacity of adsorption of ions in alkaline solutions has also been investigated [23].

Membranes are generally negatively charged, however, there are some that are positively charged; in some membranes the Donnan exclusion seems to be what determines the removal mechanism. [24]. Nanofiltration has demonstrated high effectiveness of sulphate ions removal, yielding about 98% in ideal conditions [25].

However, not always those technologies are efficient. The elimination of sulphate ions is not an easy task, due to their high solubility and stability in aqueous solutions [26]. That is why in the last years, the electrocoagulation method has been widely used for the treatment of wastewaters, as this process allows to destabilize the suspended or dissolved chemical species found in a solution. This electrochemical process is based on the application of a difference of electric potential by means of cathode-anode method (using aluminum electrodes), immersed into a solution of water to treat. As a consequence and during the course of the said electrolytic process, the cationic species, produced in the anode, come into the solution making reaction with the species and forming metallic oxides and precipitating the respective hydroxides (for the case of the sulphates) [27]. The efficiency of this method is the function of different parameters, like the difference of potential, current density, electrodes nature and pH [28].

The mechanism of sulphate ions removal by electrocoagulation is carried out through a mechanism of adsorption, in which the aluminum flocs catch the SO_4^{2-} ions. There is no chemical interaction between these ions and metal compounds of hydroxyl, but it suggests an electric interaction [29]. The objective of this work is to discuss and analyze the key operating parameters for the removal of sulphate ions from the abandoned mines, as well as the characterization of the flocs generated during the electrocoagulation process, in order to be used for future research.

Figure 2 shows the residual concentration of sulphate ions ($C_{SO_4^{2-}}$) after the electrocoagulation process as a linear speed function at current density values of 4, 5, 6 and 7 mA cm^{-2} .

The theoretical concentration of aluminum, generated within the electrocoagulation reactor, was calculated through the equation (1).

$$C_{Al^{3+}} = (N) \left(\frac{j \cdot L \cdot MW}{z \cdot F \cdot S \cdot u_r} \right) (10^6) , \tag{1}$$

where j is the current density ($A\ cm^{-2}$), L is the channel length (cm), MW is the molecular weight of aluminum ($26.98\ g\ mol^{-1}$), Z is the number of electrons exchanged ($z=3$), F is the Faraday constant ($96485\ C\ mol^{-1}$), S is the channel width (cm), u_r is the linear flow velocity ($cm\ s^{-1}$), N is the number of channels ($N=8$) and 10^6 is a conversion factor used to obtain the aluminum concentration in $mg\ L^{-1}$.

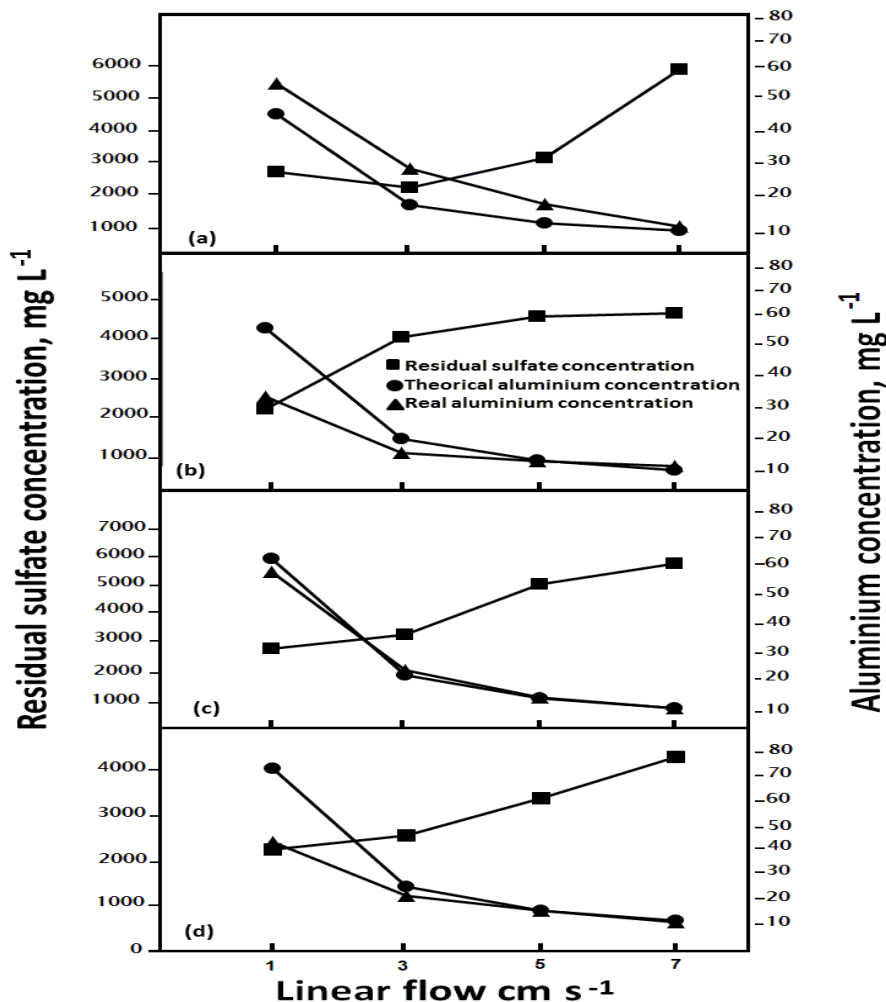


Figure 2. Influence of the linear velocity on the sulphate ions removal and the experimental and theoretical aluminum concentration in the multistage reactor for the water coming from mine after the electrocoagulation process (initial parameters: $C_{SO_4^{2-}}$ 6704 $mg\ L^{-1}$, pH 8.2, conductivity 3.72 $mS\ cm^{-1}$) and at current densities of (a) 4, (b) 5, (c) 6 and (d) 7 $mA\ cm^{-2}$.

Figure 2 shows the concentration of residual sulphate ions concentration ($C_{SO_4^{2-}}$) after the EC process as a linear velocity function at different current densities. At 4 $mA\ cm^{-2}$, $C_{SO_4^{2-}}$ decreased from

2351 to 1871 mg L⁻¹. Nevertheless, at $u_r > 4.9$ cm s⁻¹, $C_{so_4^{2-}}$ increased from 2777 to 5422 mg L⁻¹ due to the fact that both theoretical and experimental aluminum concentration decreased with the linear velocity increase; the maximum removal of sulphate ions reached 72% (1871 mg L⁻¹) with the theoretical and real concentration of aluminum of 13.61 and 24.48 mg L⁻¹, respectively.

At 5 mA cm⁻² and u_r of 0.98 cm s⁻¹, $C_{so_4^{2-}}$ was obtained with a value of 2170 mg L⁻¹, and at values of $u_r > 2.96$ cm s⁻¹, $C_{so_4^{2-}}$ increased linearly from 4034 to 4643 mg L⁻¹. The sulphate ions removal efficiency was 67.6 % (2170 mg L⁻¹).

In tests carried out at 6 mA cm⁻² and at u_r of 0.98 cm s⁻¹, a percentage of sulphate ions removal of 55 % (2974 mg L⁻¹) was obtained, with a theoretical and experimental aluminum concentration of 61.24 and 56.71 mg L⁻¹, respectively. Similar results concerning the concentration of sulphate ions after an electrocoagulation process using the abandoned mine water were presented [30, 31, 32]. For the values between $2.90 < u_r < 6.90$ cm s⁻¹, the concentration of sulphate ions increased linearly from 3450 to 5960 mg L⁻¹.

Finally, at 7 mA cm⁻² and u_r of 0.98 cm s⁻¹, we had the best concentration obtained of the residual sulphate ions, which was 2178 mg L⁻¹ with a real and theoretical aluminum concentration of 41.9 and 71.4 mg L⁻¹, respectively; the difference between the values of these concentrations is possibly due to the electrode passivation. Aluminum hydroxide precipitates are the primary species with very few amounts of soluble species for low current density and pHs around neutrality, which then aggregate to form flocs (between 5 and 9) [33-34].

It is worth mentioning that this value of $C_{so_4^{2-}}$ does not meet the maximum limit allowed by the Mexican Official Standard (< 400 mg L⁻¹); the study of the removal of sulphate ions from the mine water in order to achieve the compliance with the Mexican Official Standard is not within the objectives of this work.

When the current density increases, we can observe that the aluminum concentration increases linearly for the current densities that are equal or lower than 6 mA cm⁻²; however, at higher values (>6 mA cm⁻²), the dissolution efficiency of aluminum decreases. This behavior might be due to positive conditions that enhance water oxidation, which competes with the aluminum oxidation, equation (2) [34].



The current not only determines the coagulant dosage rate, but also the bubble production rate and fluid regime (mixing) within the reactor [35]. Electrocoagulation could be considered as a suitable auxiliary process for the removal of sulphate while treating other compounds, but not the main sulphate treatment technology.

The Energy Dispersive X-Ray Spectroscopy (EDS) analysis was used to quantify the chemical elements that make up the flocs, produced by EC. Table 3 shows the chemical composition of flocs at different current densities, which indicates on the presence of the following elements: O, Na, Mg, Al, Si, S, Cl, K and Ca. It can be observed that the chemical composition is similar to different current densities, what also coincides with what was reported in other studies results [30].

Figure 3 illustrates the IR spectrum of the flocs originated through the EC, where at a wave length from 500 to 700 cm⁻¹, there may be observed the characteristic peaks of Al – OH and Al – O vibrations;

meanwhile, at a wave length between 1000 and 1300 cm^{-1} , the peak corresponds to SO_4^{2-} vibrations. The carbonates are observed at a 3500 nm wave length.

Table 3. Chemical composition of flocs determined by EDS.

| Element | Atom average in % | | | |
|---------|-----------------------|-----------------------|-----------------------|-----------------------|
| | 4 mA cm^{-2} | 5 mA cm^{-2} | 6 mA cm^{-2} | 7 mA cm^{-2} |
| O | 67.62 | 64.08 | 63.18 | 64.63 |
| Na | 3.59 | 12.86 | 14.16 | 9.75 |
| Mg | 10.05 | 2.88 | 3.92 | 6.25 |
| Al | 2 | 0.97 | 1.22 | 1.43 |
| Si | 0.29 | 0 | 0 | 0 |
| S | 12.83 | 14.01 | 15.73 | 13.15 |
| Cl | 1.36 | 0.93 | 0.77 | 1.43 |
| K | 0.21 | 2.09 | 0.46 | 2.25 |
| Ca | 2.05 | 2.18 | 0.56 | 1.11 |

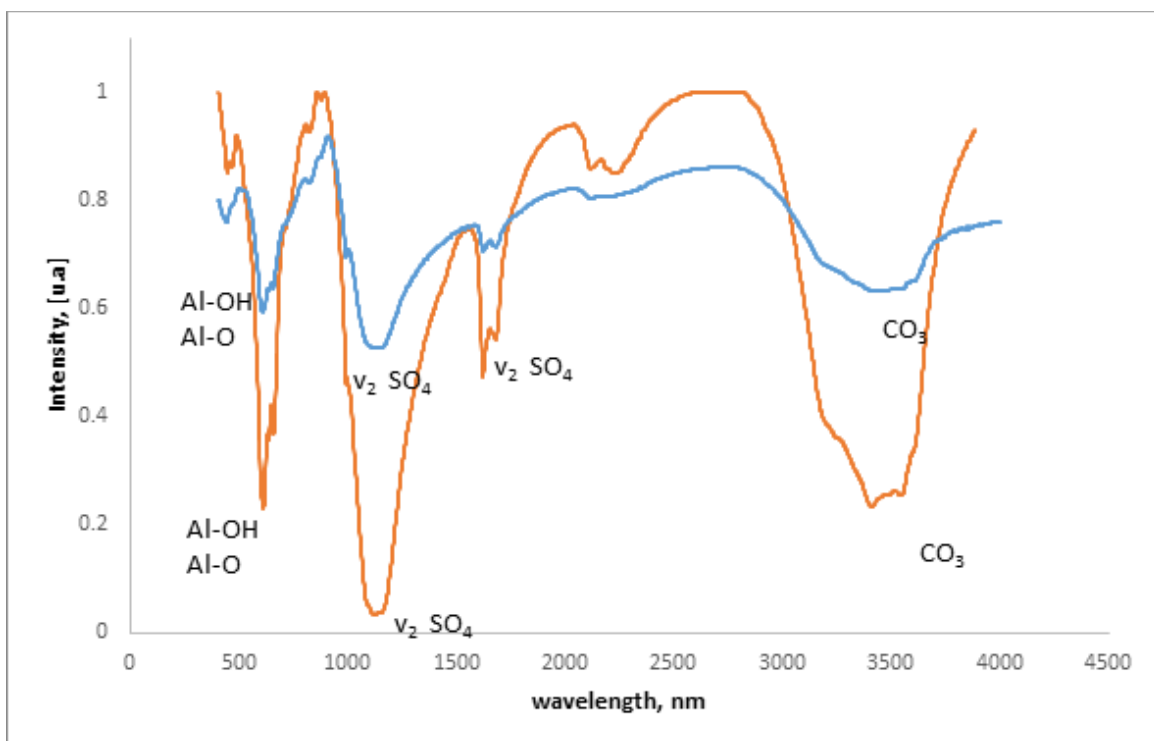


Figure 3. IR spectrum of dry flocs obtained by EC at 4 and 6 mA cm^{-2} and 0.98 cm s^{-1} .

The spectra were obtained for samples with the current density of 4 and 6 mA cm^{-2} ; it was observed that both samples had the same functional groups, i.e. they had the same chemical composition.

The morphology results and the particle size of flocs obtained through SEM are shown in Figure 4. The flocs were irregularly shaped, compact and aggregate with an average size of a particle of 5μ . The photomicrographs also show the presence of small crystals of prismatic shape that are more visible

when the current density decreases; those crystals are probably due to the presence of calcium, magnesium and sodium salts.

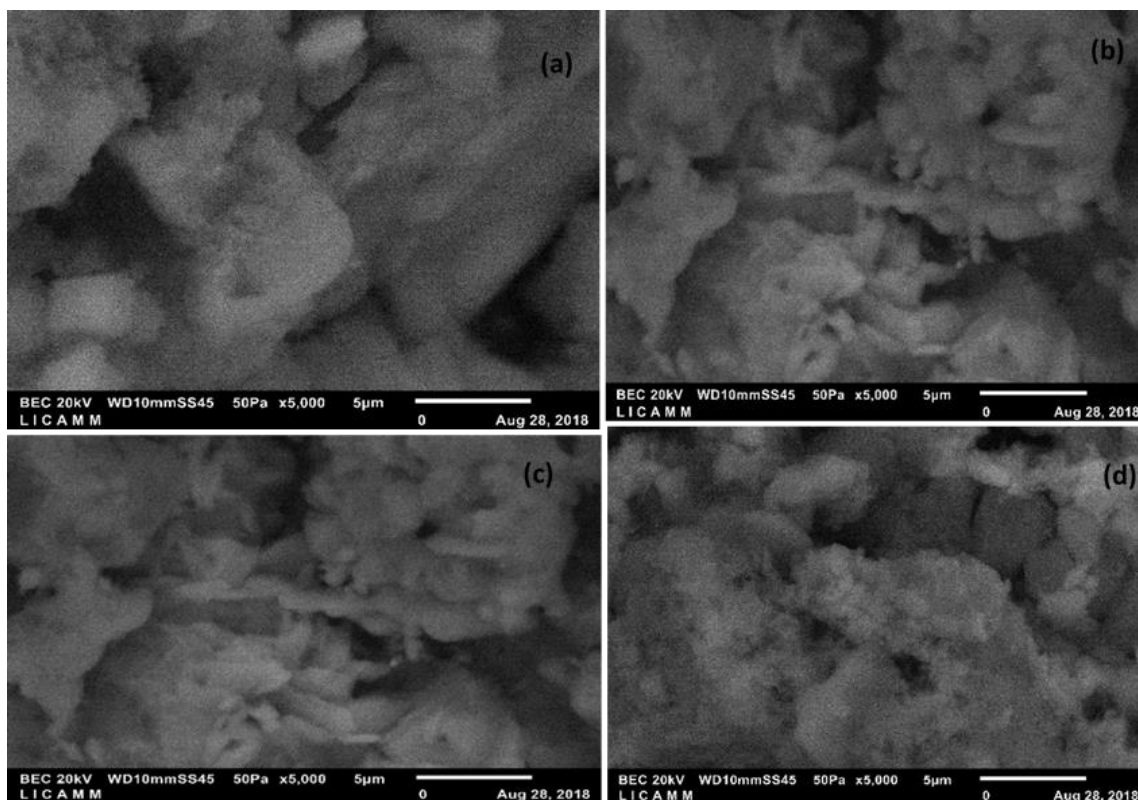


Figure 4. Photomicrographs of flocs during the EC process at current densities of (a) 4, (b) 5, (c) 6 and (d) 7 mA cm⁻² and u_r of 0.98 cm s⁻¹.

Figure 5 illustrates the X-ray diffractogram of the flocs generated in the electrocoagulation process at 4 mA cm⁻², also performed at 6 mA cm⁻², and the structure is the same; it can be observed that the material presents a high crystallinity and very marked peaks at values of 2θ between 8 and 40, which correspond to different phases, such as Gypsum, syn – CaSO₄.2H₂O, Mirabilite – Na₂SO₄.10H₂O, Gibbsite, syn – Al(OH)₃, Diaspore AlO (OH), Palygorskite Mg₅(Si,Al)₈O₂₀(OH)₂.8H₂O and Brushite CaPO₃(OH).2H₂O principally. These results were different with those reported [30], where the flocs obtained through the electrocoagulation process of sulphates, presented in the aqueous solution, were characterized. In this study, the phases using real water from a mine are reported, unlike what was reported [30], which uses synthetic water. It can also be observed that the crystalline structure does not change with the current density. The diffractograms again confirm the presence of sulphate salts and aluminum hydroxide in the flocs. These results coincide and confirm what was found with the SEM-EDS and IR analyses.

The aluminum coordination in the flocs structure was determined by the Nuclear Magnetic Resonance of Solids (RMNS) for ²⁷Al. The results obtained from RMNS for the samples at a current density of 6 mA cm⁻² and changes of the flow velocity (0.98, 2.96 and 4.93 cm s⁻¹) are shown in Figure 6. A well-defined peak is observed between 50 and 0 ppm, which corresponds to the hydrolyzed

aluminum in its tetrahedral form (Al(OH)₃); these results are consistent with the study of Kim [36] for an aluminum sample. The hydrolyzed aluminum presents a charge deficiency, which is compensated by the sulphate ions (SO₄²⁻), obtained through the electrocoagulation process, as shown in the equation 3 [29].

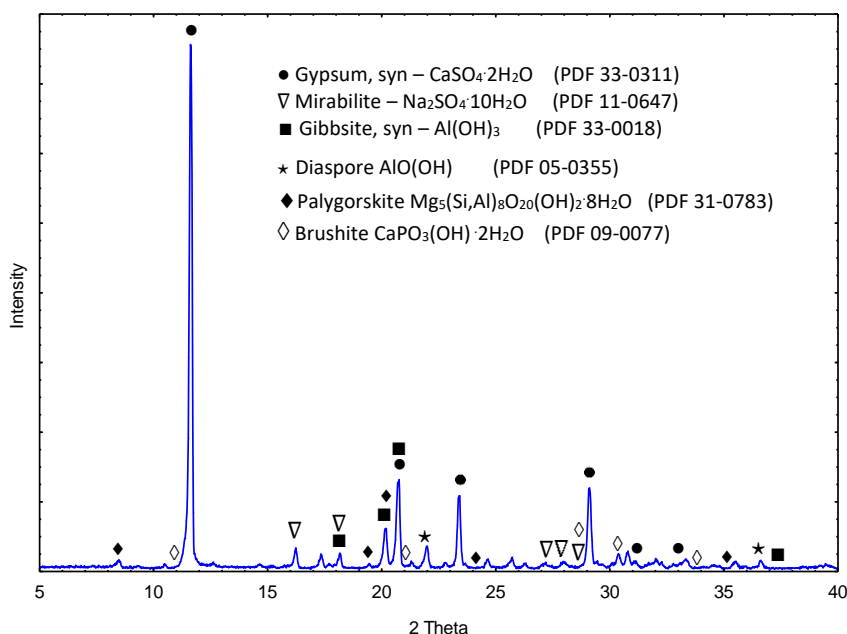
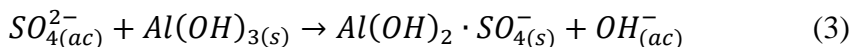


Figure 5. XRD diffractogram of dry floes obtained by EC at a current density of 4 and 6 mA cm⁻² and a flow velocity of 0.98 cm s⁻¹.

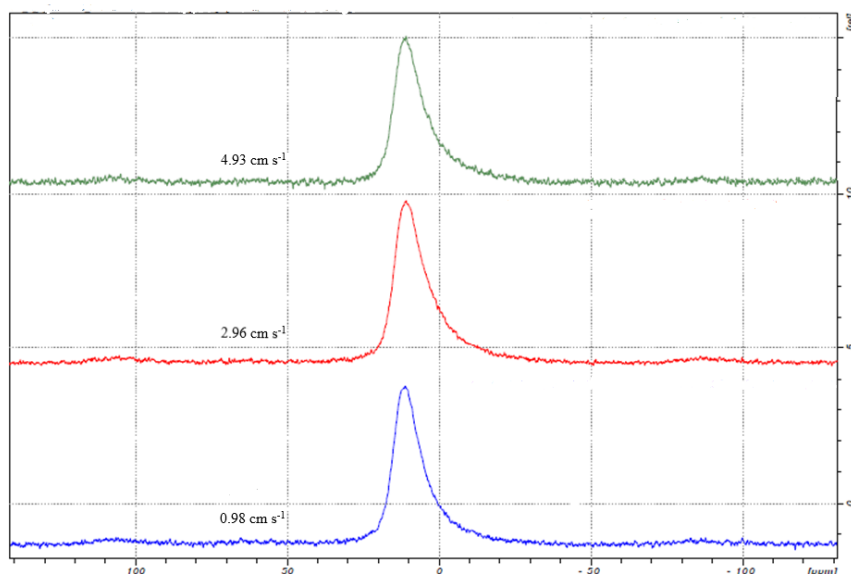


Figure 6. RMNS chart for the floes at a current density of 6 mA cm⁻² and a linear flow velocity (0.98, 2.96 and 4.93 cm s⁻¹).

4. CONCLUSIONS

In this work, we studied the process of sulphate ions removal from an abandoned mine in the city of Guanajuato, Mexico, through the electrocoagulation process; the following current densities were employed: 4, 5, 6 and 7 mA cm⁻² for a range of linear velocity of $0.98 \leq u_r \leq 2.90$ cm s⁻¹; it was observed that the concentration of sulphate ions decreased from 6704 mg L⁻¹ to 1871 mg L⁻¹ (obtaining a removal of 72%), using a current density of 4 mA cm⁻² and at a linear velocity of 2.95 cm s⁻¹.

The characterization results for the flocs obtained by EC showed that the crystalline structure and the functional groups are independent of the operating variables of the electrocoagulation process. These results allowed us to verify that the reaction mechanism between aluminum and sulphate ions is achieved by electrostatic attraction.

ACKNOWLEDGMENTS

Brett González thanks CONACYT for the scholarship 46047. We also thank Daniela Moncada from LICAMM-UG laboratory for her help in SEM and XRD analysis; Iris Cervantes and Rebeca Perez from Chemistry Department-UG for their help in infrared spectrometry and UV-Visible Spectroscopy analysis. Thanks to the Engineering Department in Mines, Metallurgy and Geology of the Engineering Division of the University of Guanajuato for allowing access to “The Nopal” mine to take water.

References

1. E. López, O. Aduvire and D. Baretino, *Bol. Geol. Miner.*, 113 (2002) 3.
2. O. Aduvire and H. Aduvire, *Ingeopres*, 141 (2005) 52.
3. W. M. Ashane, I. Ilankoon, T. Syed and M. Yellishetty, *Miner. Eng.*, 117 (2018) 74.
4. K. Hogsden and J. Harding, *Freshw. Sci.*, 31(2012) 108.
5. D. DeNicola and M. Stapleton, *Environ. Pollut.*, 119 (2002) 303.
6. G. Skousen, F. Ziemkiewicz and L. McDonald, *Extr. Ind. Soc.*, 6 (2019) 241.
7. R. W. Gaikwad and D. V. Gupta, *Appl. Ecol. Environ. Res.*, 6 (2008) 81.
8. J. García and A. Barabas, *Geomimet*, 207 (1997) 13.
9. (<http://ciudadmuseo-gto.com/mina-del-nopal>, access 15 November 2018).
10. V. Preuß, C. Riedel, T. Koch, K. Thürmer and M. Domańska, *Arch. Civ. Eng. Environ.*, 3 (2012) 127.
11. M. Khorasanipour, F. Moore and R. Naseh, *Mine Water Environ.*, 30 (2011) 216.
12. D. B. Johnson and K.B. Hallberg, *Sci. Total Environ.*, 338 (2005) 3.
13. Moodley, C. Sheridan, U. Kappelmeyer and A. Akcil, *Miner. Eng.*, 126 (2018) 139.
14. J. Rubio, M. L. Souza and R. W. Smith, *Miner. Eng.*, 15 (2002) 139.
15. D. Guimarães and V.A. Leão, *J. Hazard. Mater.*, 280 (2014) 209.
16. R. Haghsheno, A. Mohebbi, H. Hashemipour and A. Sarrafi, *J. Hazard. Mater.*, 166 (2009) 961.
17. D. Feng, C. Aldrich A. and H. Tan, *Miner. Eng.*, 13 (2000) 623.
18. A. Akcil and S. Koldas, *J. Clean Prod.*, 14 (2006) 1139.
19. X. Tian, Z. Zhou, Y. Xin, L. Jiang, X. Zhao, and Y. An, *J. Hazard. Mater.*, 365 (2019) 572.
20. E. T. Tolonen, J. Rämö and U. Lassi, *J. Environ. Manage.*, 159 (2015) 143.
21. S. Hong, F. S. Cannon, P. Hou, T. Byrne and C. Nieto-Delgado, *Chemosphere*, 184 (2017) 429.
22. H. Runtti, P. Tynjälä, S. Tuomikoski, T. Kangas, T. Hu, J. Rämö and U. Lassi, *J. Water Process. Eng.*, 16 (2017) 319.
23. E. Iakovleva, E. Mäkilä, J. Salonen, M. Sitarz and M. Sillanpää, *Chem. Eng. J.*, 259 (2015) 364.
24. J. M.M. Peeters, J.P. Boom, M.H.V. Mulder and H. Strathmann, *J. Membr. Sci.*, 145 (1998) 199.
25. K. Ambiado, C. Bustos, A. Schwarz and R. Bórquez, *Water Sci. Technol.*, 75 (2017) 705.

26. M. Mamelkina, S. Cotillas, E. Lacasa and M. Rodrigo, *Sep. Purif. Technol.*, 182 (2017) 87.
27. K. Savas and U. Ogutveren, *J. Hazard. Mat.*, B89 (2002) 83.
28. S. García, M. Maesia, J. Vieira de Melo and C. A. Martínez, *J. Electrochem. Sci. Technol.*, 801 (2017) 267.
29. Q. Zuo, X. Chen, W. Li and G. Chen, *J. Hazard. Mater.*, 159 (2008) 452.
30. M. Sandoval, J.L. Nava, O. Coreño, G. Carreño, L. A. Arias and D. Mendéz, *Int. J. Electrochem. Sci.*, 12 (2017) 1318.
31. P. Del Ángel, G. Carreño, J. L. Nava, M. T. Martínez and J. Ortiz, *Int. J. Electrochem. Sci.*, 9 (2014) 710.
32. E. Nariyan, A. Aghababaei and M. Sillanpää, *Sep. Purif. Technol.*, 188(2017) 266.
33. W. Yu, L. Xu, K. Lei and J. Gregory, *Water Res.*, 143 (2018) 346.
34. C. Jiménez, C. Sáez, F. Martínez, P. Cañizares and M. Rodrigo, *Sep. Purif. Technol.*, 98 (2012) 102.
35. P. Holt, G. Barton, M. Wark and C. Mitchell, *Colloids Surf. A.*, 211 (2002) 233.
36. Y. Kim, *Chemosphere*, 119 (2015) 803.

© 2019 The Authors. Published by ESG (www.electrochemsci.org). This article is an open access article distributed under the terms and conditions of the Creative Commons Attribution license (<http://creativecommons.org/licenses/by/4.0/>).